9-16-2014

Long-lasting effect of initial configuration in gravitational spreading of material fronts

Nadim Zgheib

Thomas Bonometti

S. Balachandar

Nadim Zgheib · **Thomas Bonometti** · **S. Balachandar**

Long-lasting effect of initial configuration in gravitational spreading of material fronts

Abstract We present the results from laboratory experiments and fully resolved simulations pertaining to finite-release turbulent density flows with a non-axisymmetric initial shape. First, we demonstrate that the effects of the initial shape influence the current's evolution well into the long-time phase which would corresponds to the inertial self-similar phase in the case of planar or axisymmetric configurations. Then, we identify the physical mechanisms responsible for this dependence and propose a new model capable of capturing the dynamics of such releases. Finally, we show that this dependence on the initial configuration is robust for various types of gravity currents over a wide range of parameters such as Reynolds number, density ratio, and aspect ratio.

Keywords Density currents · Gravity currents · Buoyancy-driven flows · Box model · Spectral methods

1 Introduction

Consider an accidental collapse or a skilled demolition of a building vertically on itself. The emerging debris cloud will quickly invade a wider region that greatly surpasses the bounds of the demolished building. During the infamous 9/11 attack, the tidal wave of dust and debris enveloped much of the lower Manhattan. The gravitational spreading of these destructive debris clouds, as seen in Fig. 1, sensitively depends on the building's shape. The non-axisymmetric nature of the resulting lobe-like structure is persistent over a significant time and cannot be predicted by current models. This counter-intuitive behavior of initial condition-dependent spreading of material fronts is not unique to debris clouds and is applicable to a variety of geophysical flows as demonstrated in this paper. Debris clouds belong to the family of gravity currents which are observed in various natural situations. The manner in which these flows spread has important implications for oil spills [1], accidental toxic gas releases [2,3], fire propagation [4], turbidity currents [5], pyroclastic flows [6], avalanches

N. Zgheib · S. Balachandar
Department of Mechanical and Aerospace Engineering, University of Florida, Gainesville, FL 32611, USA
E-mail: nzgheib@gmail.com

S. Balachandar
E-mail: bala1s@ufl.edu

N. Zgheib · T. Bonometti (✉)
Université de Toulouse, INPT, UPS, UMR 552, IMFT, Allée Camille Soula, 31400 Toulouse, France
E-mail: thomas.bonometti@imft.fr

T. Bonometti
CNRS, IMFT, 31400 Toulouse, France

Fig. 1 Field observations of a non-circular gravity current. Aerial views of (*top*) a building of square cross section and (*bottom*) a T-shaped building being demolished. The structure of the debris cloud is highly dependent on the building's shape. Observe that material very close to the center of the building moves farther out than material located at the building's extremities. The dynamics of the cloud is reasonably well captured by our proposed model, where the front location of the cloud is marked at equal instants of time as *blue lines* (color figure online)

[6,7] and storms [8]. These flows are driven by a difference in density either stemming from temperature, salinity or suspended sediments.

Predicting the short-time as well as long-time evolution of these material fronts is of crucial interest [9,10]. Most real gravity currents are generated by a sudden or continuous release from an arbitrary, often non-circular, source. However, nearly all the prior theoretical, experimental and numerical investigations are based on planar or axisymmetric configurations [11–14]. The underlying (implicit) assumption is that, after a relatively short transitional phase, the material front becomes either planar or axisymmetric. Here, we present results from laboratory and numerical experiments that were performed with non-axisymmetric finite initial releases. The most striking feature was that the effect of the initial non-circular shape of the release persists for the whole duration of the observation. This is a unique, but robust, behavior of propagating material fronts, which is quite distinct from propagating informational fronts, such as sound waves and shock fronts, which are well known to quickly become independent of the source shape.

In the present paper, we identify the physical mechanisms responsible for this peculiar behavior and present a novel model which accounts for the shape of the initial release and predicts the non-axisymmetric propagation of the front of the gravity current. This model when applied to the problem of building demolition captures the time evolution of the observed debris cloud (Fig. 1).

2 Non-circular spreading of density currents

When a patch of heavy (resp. light) fluid spreads in a lighter (resp. heavier) ambient, it generally goes through successive stages [15,16], namely an acceleration phase at the end of which the current's front velocity reaches its maximum value, a slumping phase with constant or nearly constant front velocity, and eventually a phase denoted here as long-time phase where the buoyancy driving force is balanced either by inertia, viscosity or surface tension, respectively. Note that the long-time phase is often referred to as self-similar phase, because it is possible to find an exact long-time similarity solution of the simplified equations of motion (e.g., the shallow-water equations) in some specific configurations as in the planar or axisymmetric case. When a self-similar solution exists, the time evolution of the front height h_N and front velocity u_N usually follows the scaling law $h_N \sim t^\alpha$ and $u_N \sim t^\beta$ with α and β being some constants. For instance, in the case of axisymmetric gravity currents, the one-layer shallow-water equations give $\alpha = -1$ and $\beta = -1/2$. The reader is referred to the work [17,23] for more details about the existence of a similarity solution in various configurations.

While the slumping and self-similar phases have been extensively studied in the past [1,12,15,16,18,19], the initial acceleration phase has received very little attention [16,20] as initial conditions were believed to be unimportant in the prediction of the long-term dynamics. Here, we argue, by means of experiments and fully
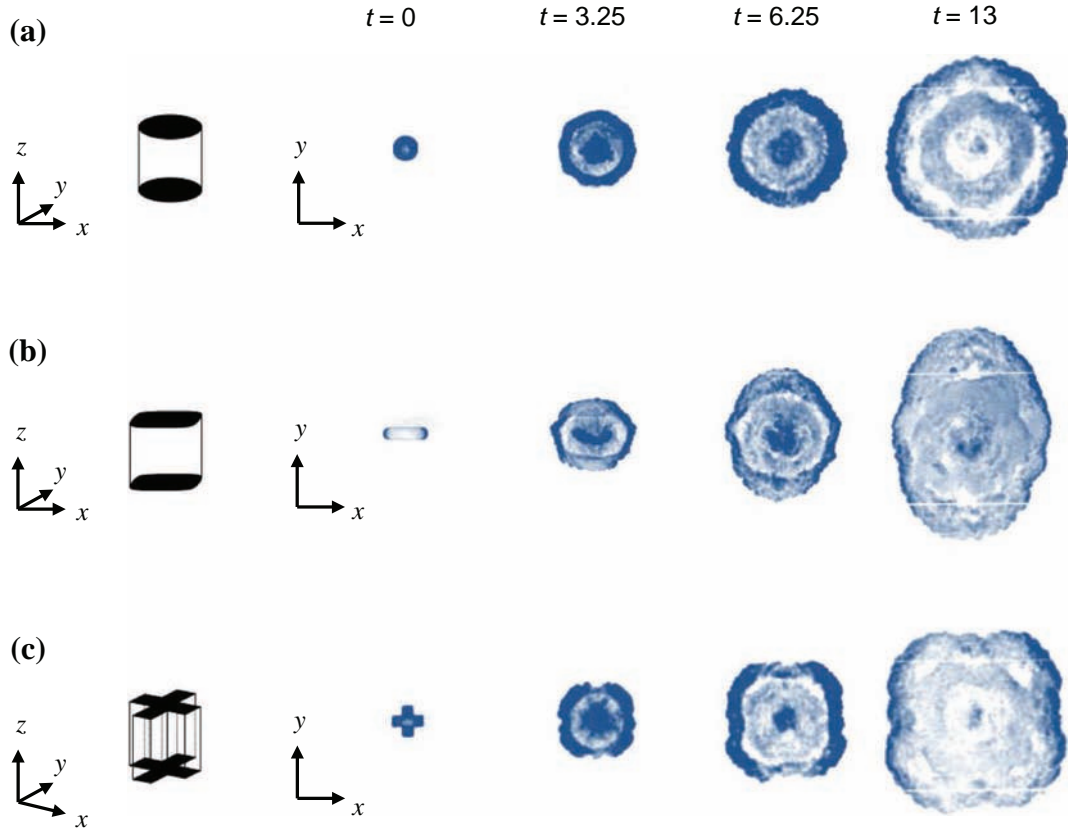
Fig. 2 Temporal evolution of the experimental collapse of a column of salt water with different cross sections at the center of a tank containing fresh water ($H/R_0 = 2$, $Re = 2.8 \times 10^4$, $\rho_c/\rho_a = 1.1$). The schemes on the left depict the three-dimensional initial shape of the heavy material in the experiment, namely cylinders of **a** circular, **b** rounded-rectangle and **c** plus-shaped cross sections. Gravity is oriented opposite to z axis. Time is scaled by $T = H/U$ (see text for definition)

resolved simulations, that a non-axisymmetric finite-volume release does not reach an axisymmetric shape nor preserves its initial shape for a significant time. In the following, we define the "long-time" regime as the regime for which the current has entered a phase for which the local front height and speed obey a scaling law of the form $h_N \sim t^\alpha$ and $u_N \sim t^\beta$, as found for the self-similar (inertial) phase.

The laboratory experiments consist of swiftly releasing a column of dense salty water ($\rho_c \approx 1,100$ kg/m^3) of height h_0 into a lighter ambient fluid of height H inside a $1.2 \times 1.2 \times 0.4$-m tank, thanks to a hollow cylinder of equivalent radius R_0. The ambient fluid is either clear water ($\rho_a \approx 1,000$ kg/m^3) or air ($\rho_a \approx 1.2$ kg/m^3). Unless stated otherwise, we set $h_0 = H$ (full-depth release). Three different cross-sectional shapes are considered: (a) a circular section, (b) a rounded rectangular section, i.e., a rectangle where the two shorter edges are replaced by semicircles, and (c) a plus-shape section for which concave corners are present (see e.g., Fig. 2). Fluorescent dye is added to the fluid inside the cylinder. The front location and the current's height are measured thanks to a mirror placed beneath the tank, which allows for a plan (bottom) view of the front evolution, while the side view of the current provides information about the height's evolution.

Several experiments have been performed for a wide range of Reynolds number $Re = HU/\nu$ ($U = [g(\rho_c - \rho_a)H/\rho_a]^{1/2}$ being the velocity scale, g the gravitational acceleration, and ν the kinematic viscosity of water), initial height aspect ratio H/R_0, and density ratio ρ_c/ρ_a. As seen in Table 1, the initial aspect ratio based on the local distance from the center of mass is in the range 0.5–8.5, covering both configurations of $O(10^{-1})$ and $O(10^1)$ aspect ratio. In all cases, the flow was fully turbulent. The commonly accepted distance of propagation for which transition from the slumping phase to the inertial self-similar phase occurs is about 2 (resp. 5–9) in the cylindrical (resp. planar) configuration [18,24]. Here, the distance of propagation was in the range 7–25; hence, the current is likely to enter a regime which resembles the self-similar phase in all cases so the "long-time" regime is reached, as it will be confirmed later (Figs. 3, 4).

Table 1 Parameters used in the experiments and/or simulations

Reynolds number	Re		
	$[7 \times 10^3, 10^6]$		
Initial depth ratio	H/h_0		
	1–2		
Initial aspect ratio	$H/R_{\max}$	H/R_0	$H/R_{\min}$
	0.5	1–2–4	8.5
Density ratio	ρ_c/ρ_a		
	$0.93–1.1–10^3$		
Distance of propagation	$L/R_{\max}$	L/R_0	$L/R_{\min}$
	7	12	25

$h_0(H)$ is the initial height of the current (ambient), R_0, $R_{\min}$, $R_{\max}$ are the initial equivalent, minimum, maximum radius of the cross-sectional area of the cylinders, L is the maximum distance of propagation

As mentioned above, the behavior of material fronts is in stark contrast to propagation of information (or wave) fronts. For example, an outward propagating sound wave front quickly becomes spherical irrespective of the shape of the source [21] and the front radius is linearly related to time through sound speed as $r = c_0 t$ (note that sound intensity distribution depends on the source detail). Similarly, a blast wave from a finite source quickly becomes spherically independent of the source shape. Here, again the blast radius can be expressed by the power law [22] $r \sim t^{2/5}$. Although the blast front velocity decreases with time, it remains the same along the entire blast front. Clearly, the propagation of a material front, e.g., gravity currents, cannot be modeled as that of an information front.

The temporal evolution of some axisymmetric and non-axisymmetric gravity currents is presented in Figs. 2, 3 and 4. When the release is non-circular, the current's evolution depends on the initial shape within the time of the observation. For instance, in the case of the gravity current of initial rounded-rectangle cross section, the local front velocity and height at the tips of the initial major (slow) and minor (fast) axes (see the marks S and F in Fig. 7) show large differences in magnitude early after material redistribution (see Figs. 3, 4, $t > 2$). Over time, the magnitude of the difference somewhat decreases, but persists up to the end of the experiment/simulation, indicating that the current has not become axisymmetric nor reverted back to its original shape within the limited time of observation. For instance, the patch of heavy fluid of initial rounded-rectangle shape is observed to flip axes, while that of initial plus shape turns into a square.

Initially, the height of the patch is uniform across the surface, and hence, the pressure force is the same along the current's front. As a consequence, just after release, the current rapidly accelerates outward with increasing speed, but initially the current's speed u_N and height h_N are independent of the initial shape and are uniform around the circumference of the front (see Figs. 3, 4 for $t < 1$). Upon the release of the heavy fluid inward propagating perturbations initiate at the front, which reflect back at the center of the patch and eventually catch up to the front [23]. During the acceleration phase, the heavy material is redistributed within the patch following the direction perpendicular to the initial front. At the end of the redistribution phase, the height h_N is not uniform along the front of the current (Fig. 3, $t \approx 2$). Since the front velocity u_N scales as $\sqrt{h_N}$ (see e.g., Ref. [10,15]), the speed of propagation is non-uniform along the current's front. This non-uniform circumferential distribution of the heavy fluid within the current, as dictated by the initial shape, remains fixed over time leading to a non-axisymmetric spreading of the current during the slumping and the subsequent spreading phase of the current.

For comparison, the time-dependent solution of the axisymmetric one-layer shallow-water equations (equations 6.24–6.25 in Ref. [23]) obtained with a finite-difference method similar to that described in appendix 2 of [23] is plotted in Figs. 3b and 4b together with the fully resolved simulation and experimental results. Figure 3b shows that the temporal evolution of the local front height of the gravity current of initial rounded-rectangle cross section roughly follows a slope -1 in log–log representation at times larger than $t \approx 5$ approximately. The same trend is observed for the time-dependent solution of the one-layer axisymmetric shallow-water equations at a somewhat earlier time $t \approx 3$. Similarly, the local front speed in Fig. 4b is observed to roughly follow a slope $-1/2$, as clearly seen for the experimental local "fast" front speed. Note that some fluctuations are present in the evolution of the local "slow" front speed, making the comparison more difficult. Comparing the temporal evolution of the local front speed of the non-axisymmetric gravity currents with the time-dependent solution of the one-layer axisymmetric shallow-water equations indicates that the non-axisymmetric gravity
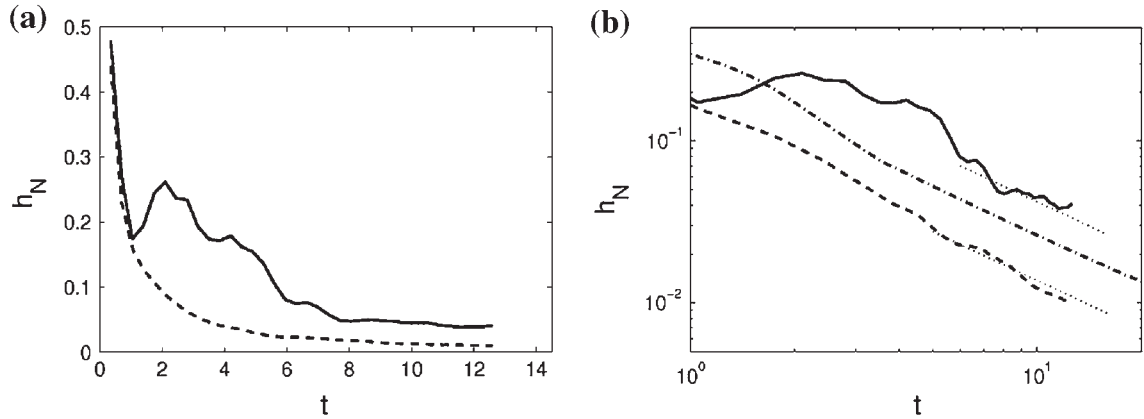
Fig. 3 Temporal evolution of the local front height in the vertical mid-plane of x direction (*dashed line*) and y direction (*solid line*) of the current of initial rounded-rectangle cross section. **a** Results obtained from the fully resolved simulation with $H/R_0 = 2$ and $Re = 8,950$. **b** Same as (**a**) in log–log representation. For comparison, the time-dependent solution of the axisymmetric one-layer shallow-water equations using Huppert and Simpson's [15] front condition in the full-depth configuration is shown in (**b**) (*dash-dot line*). The *dotted lines* indicate a slope of -1, as predicted by the self-similar solution of the axisymmetric one-layer shallow-water equations (see e.g., Ref. [23, p. 122])
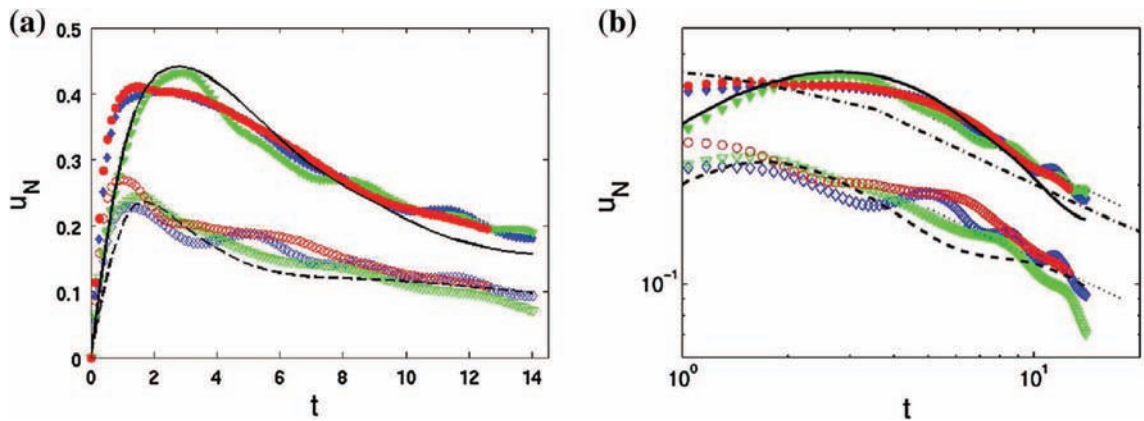

Fig. 4 Temporal evolution of the local front speed in the vertical mid-plane of x direction (*lower curves*) and y direction (*upper curves*) of the current of initial rounded-rectangle cross section. **a** The *solid* and *dashed lines* correspond to results obtained from the fully resolved simulation with $H/R_0 = 2$ and $Re = 8,950$, while the *symbols* are from three experiments for which $H/R_0 = 2$ and $Re = 2.8 \times 10^4$. **b** Same as (**a**) in log–log representation. For comparison, the time-dependent solution of the axisymmetric one-layer shallow-water equations using Huppert and Simpson's [15] front condition in the full-depth configuration is shown in (**b**) (*dash-dot line*). The *dotted lines* indicate a slope of $-1/2$, as predicted by the self-similar solution of the axisymmetric one-layer shallow-water equations (see e.g., Ref. [23, p. 122])

currents have entered a long-time phase which resembles the self-similar regime of the axisymmetric configuration, in that the local height and speed roughly follow a law of the type $h_N \sim t^\alpha$ and $u_N \sim t^\beta$, with α and β being some constants. Note, however, that determining the precise value of α and β, and the time at which the long-time regime starts is difficult with the present set of experimental and numerical data because of the significant velocity fluctuations observed in Fig. 4b and the somewhat limited range of parameters investigated here. Larger-size experiments and/or simulations would help to clarify this point.

The dependence of material front propagation on initial condition of release is robust in the sense that the peculiar behavior observed in Fig. 2 is not restricted to the presently discussed configurations (rounded-rectangle and plus-shaped cross sections; Boussinesq currents of density ratio close to unity). We have conducted many more laboratory and numerical experiments of different non-axisymmetric geometries, density ratios ρ_c/ρ_a (including Boussinesq currents $\rho_c/\rho_a \approx 1$, heavy currents of dam-break flow type $\rho_c/\rho_a = O(10^3)$, and light currents $\rho_c/\rho_a < 1$), different aspect ratio releases (radius to height ratio ranging between 0.5 and 7), and Reynolds numbers (see Table 1). We found that provided the Reynolds number is large enough, say $Re \geq O(10^3)$, the initial shape of the current always influences the current's continued propa-
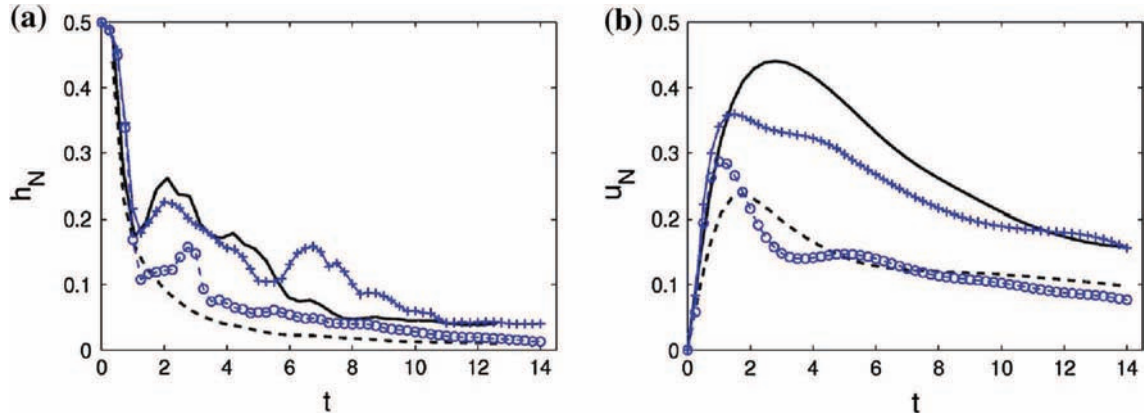
Fig. 5 Temporal evolution of the local front's height (**a**) and speed (**b**) in the vertical mid-plane of x direction (*dashed lines*) and y direction (*solid lines*) of the current of initial rounded-rectangle cross section for two initial depth ratios, namely a partial-depth release $h_0 = H/2$ (*blue lines with symbols*) and a full-depth release $h_0 = H$ (*black lines without symbols*). These results are obtained from fully resolved simulations with $H/R_0 = 2$ and $Re = 8{,}950$ (color figure online)

gation as well as its preferred asymptotic non-axisymmetric shape for a significant amount of time. Finally, we performed simulations of both full-depth and partial-depth releases (Fig. 5) and found a qualitative similar dynamics. This indicates that the presently observed behavior is independent of the initial depth ratio. Note that we performed simulations for only two values of h_0/H. Other experiments or simulations for a wider range of depth ratios would help in quantitatively determining the influence of this parameter on the dynamics of non-cylindrical gravity currents.

3 A new model for the prediction of the propagation of non-circular density flows

This finding has several theoretical implications. The classical box model, which is classically used for predicting the evolution of gravity currents [15], despite its simplicity, is able to reproduce the dynamics of axisymmetric and planar releases. However, straightforward application of the box model fails for non-axisymmetric releases (Fig. 7). According to this model, the height remains uniform along the entire spreading patch, so the speed of propagation remains uniform along the current's front during all the phases of spreading (recall that the local speed of propagation evolves as the square root of the local height of the current). Using the classical box model, an initially non-axisymmetric current inevitably becomes axisymmetric. Similarly, theories based on slumping and self-similar phases also fail to predict the sensitive dependence on the initial shape and the preferential propagation of non-axisymmetric gravity currents for the same reasons.

Fully resolved simulations support the experimental findings (Figs. 3, 4, 5, 6). The simulations are performed using a spectral code [24] to solve the Navier–Stokes equations using the Boussinesq approximation $\rho_c/\rho_a \approx 1$. The numerical domain consists of a Cartesian parallelepiped (length $\times$ width $\times$ height = $15 \times 15 \times 1$), with a spatial resolution of $880 \times 880 \times 179$ (140 million degrees of freedom). Boundary conditions are no-slip at the bottom wall, free-slip at the top, and periodic at the sidewalls. The propagation of the current front is visualized via iso-contours of the vertically averaged dimensionless density field $\rho = (\rho^* - \rho_a)/(\rho_c - \rho_a) = 0.001$ (ρ^* is the dimensional local density). Quantitative agreement is found between experiments and fully resolved simulations. The undulations seen in Fig. 6 for both simulations and experiments at later times are due to the lobe and cleft instability [25].

Even though such simulations are able to reproduce the peculiar dynamics of non-axisymmetric gravity currents, they are unlikely to be used for rapid prediction, as needed in operational models especially those dealing with the high-Reynolds numbers gravity currents.

Here, we propose an extended box model based on partitioning of the initial release using geometric rays that are perpendicular to the front (Fig. 7). Once the various subvolumes are obtained, the local fronts are advanced normal to themselves as in the box model. This initial partitioning is the key aspect of the present model, since it allows for non-uniform height and speed along the patch's advancing front, during all the phases of spreading. This allows the model to capture the non-axisymmetric propagation of the front. To be explicit, the formulation of the extended box model makes use of a Benjamin-type boundary condition (1) relating the outward normal front velocity u to the front height h, kinematic relations (2–3) for the advancement of the
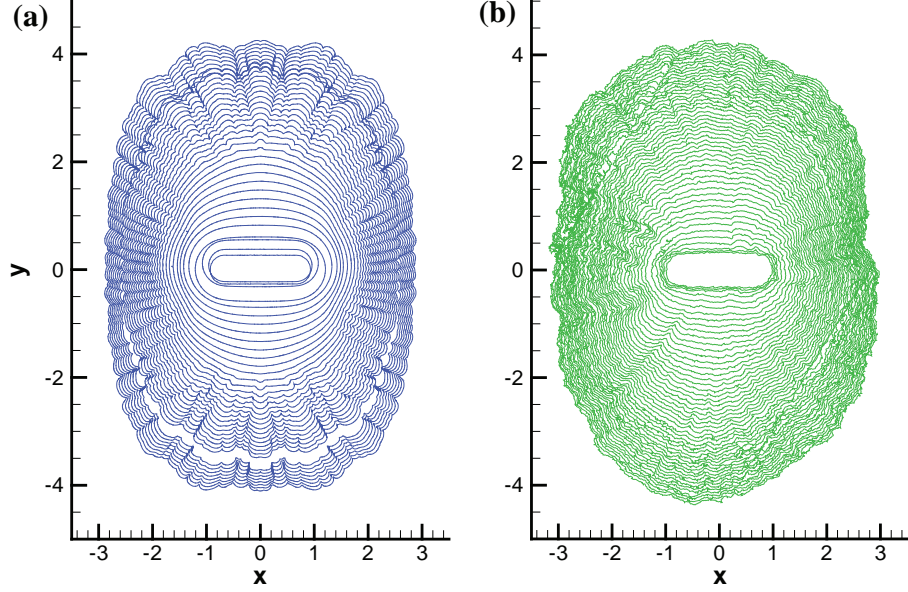
Fig. 6 Temporal evolution of a non-axisymmetric material front (fully resolved simulation vs. experiment). The initial cross-sectional geometry is a rounded rectangle. **a** Numerical simulations with $Re = 8,950$. Time separation between contours is $\Delta t = 0.35$ and the final time is $t_f = 12.6$; **b** laboratory experiments. Here, $Re = 28,000$, time separation between contours is $\Delta t = 0.26$, and the final time is $t_f = 12.73$

front position (x, y) and horizontal area per arc length σ, respectively, and mass conservation (4). This results in a system of coupled nonlinear PDEs for the unknowns u, x, y, σ and h, viz

$$u = Fr\sqrt{h} \tag{1}$$

$$\frac{\partial\{x, y\}}{\partial t} = u\frac{\{\partial y/\partial s, -\partial x/\partial s\}}{[(\partial x/\partial s)^2 + (\partial y/\partial s)^2]^{1/2}} \tag{2}$$

$$\frac{\partial\sigma}{\partial t} = u \tag{3}$$

$$\frac{\partial\sigma h}{\partial t} = 0 \tag{4}$$

where, here, Fr is the Huppert–Simpson Froude number[1] (see [15]). Note that since the flow is incompressible and entrainment is neglected, the area per arc length σ and the current height h is such that the total volume V of the current is given by

$$V = \int_s \sigma h \, \mathrm{d}s \tag{5}$$

The independent variables s and t denote the curvilinear coordinate along the front and time, respectively.

The solution to (1)–(4) is far easier and faster than the direct numerical simulations displayed in Fig. 6a. As shown in Figs. 1 and 7, the solution of the extended box model is capable of capturing the propagation of currents with arbitrary initial forms.

At this point, we have shown that (i) fully resolved simulations and (ii) the proposed extension of the box model were able to reproduce the observed propagation of non-axisymmetric gravity currents contrary to the classical box model. It is of major interest, however, to assess the capability of approaches based on the shallow-water equations to reproduce such a dynamics. This would require the development of a numerical approach for solving the two-dimensional one-layer (or better yet two-layer) shallow-water equations as done for example in [26]. The development of such an approach is, however, a non-trivial undertaking, which is

---

[1] Note that another model of Froude number function could be used without losing generality, provided this function is valid for the whole range of height ratio of nose to ambient h/H, this ratio being here in the range $0 \leq h/H \leq 1$.

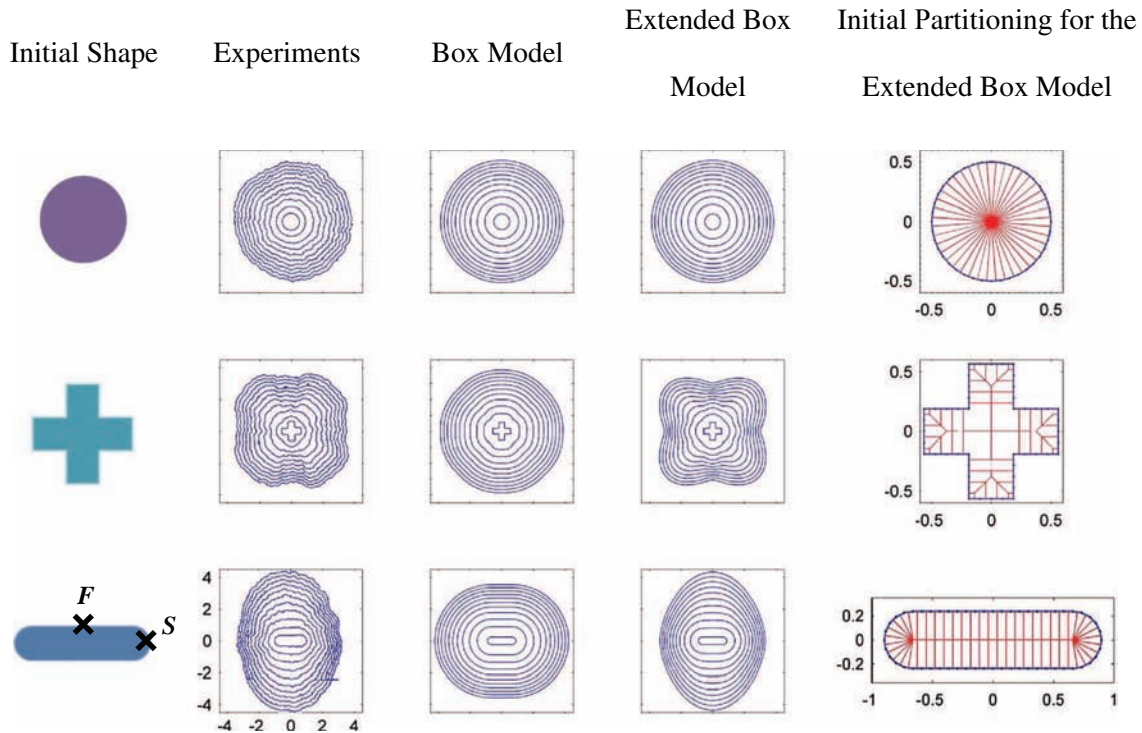| Initial Shape | Experiments | Box Model | Extended Box Model | Initial Partitioning for the Extended Box Model |

Fig. 7 Experiments versus box model/extended box model. Front location with a time separation between contours of $\Delta t = 1.3$, and a final time of $t_f = 13$. In the classical box model, as the current propagates, the height is intrinsically averaged over the entire patch of fluid making the propagation inevitably axisymmetric. In the extended box model, the volume of release is initially divided into multiple subvolumes. The size of each subvolume depends on the inwardly propagating geometric rays starting from and perpendicular to the current's front. The extended box model is in quantitative agreement with experiments, contrary to the classical box model. The marks S and F refer to the tips of the initial major (slow) and minor (fast) axes from which the front velocity and height are computed in Figs. 3 and 4

beyond the scope of the present work. Comparing the present results with a one- and/or two-layer shallow-water approach would allow clarifying the capabilities of shallow-water approaches within the hierarchy of available models for the description of non-axisymmetric gravity currents.

4 Summary and discussion

We have presented results from laboratory experiments and numerical simulations of the propagation of turbulent material fronts stemming from non-axisymmetric finite initial releases. It is found that the effect of the initial non-circular shape of the release persists for the whole duration of the observation. The duration of the experiments was such that the gravity currents have crossed a distance of 12–25 times the initial radius, if one considers the equivalent or minimum radius, respectively. This allowed to cover the acceleration phase, the (quasi-)slumping phase and a regime for which the dynamics resembles the self-similar inertial phase predicted by the one-layer axisymmetric shallow-water equations. Finally, we presented a novel model, extending the classical box model, which accounts for the shape of the initial release and predicts the non-axisymmetric propagation of the front of the gravity current.

It is important to note that the local speed of propagation of a material front generated by the release of a patch of arbitrary shape can vary significantly, thus leading to local "fast fronts" and "slow fronts." In Fig. 4, the fastest front is twice as fast as the slowest front during all the observed phases of spreading. Such long-lasting speed variations between the different sections of the front may result in dramatically different front locations that depend on the shape of the initial release. In the context of massive oil spills such as that the Deepwater Horizon oil spill stemming from the explosion of a sea-floor oil gusher in the Gulf of Mexico in April 20, 2010, the flow is likely to remain turbulent for longer times contrary to more moderate oil spills generated by tankers running aground, for which the gravity current is likely to be dominated by viscous and subsequently

capillary effects after an hour approximately [1]. In the former case, the error made in the estimation of the propagation of the oil spill front, which depends on the nature of initial release, unavoidably decreases the predictive capability of the precise location of impact along the coast. Clearly, many other factors, such as currents, cross flows, bottom topology, further influence the propagation of non-axisymmetric gravity currents. In light of the present findings, suitable additions to the extended box model described here can help improve the prediction of such gravity currents of arbitrary shapes.

Finally, it must be stressed that the present experiments/simulations were done for a limited range of parameters and on a limited spatial domain. The initial shape of the non-cylindrical gravity currents was found to influence the dynamics during the whole but limited duration of observation. For very large domains, however, non-cylindrical finite-release gravity currents are likely to enter, after some time, a regime where viscous effects are predominant. In that case, viscous diffusion of momentum may homogenize the front height and velocity so that the viscous current may become axisymmetric. More experiments on larger domains are needed to clarify whether the presently observed behavior holds for longer distances of propagation and corresponding times than those attained here.

References

1. Hoult, D.P.: Oil spreading in the sea. Annu. Rev. Fluid Mech. **4**, 341 (1972)
2. Britter, R.E.: Atmospheric dispersion of dense gases. Annu. Rev. Fluid Mech. **21**, 317 (1989)
3. Gröbelbauer, H.P., Fanneløp, T.K., Britter, R.E.: The propagation of intrusion fronts of high density ratio. J. Fluid Mech. **250**, 669 (1993)
4. Doyle, J., Carlson, J.M.: Power laws, highly optimized tolerance, and generalized source coding. Phys. Rev. Lett. **84**, 5656 (2000)
5. Meiburg, E., Kneller, B.: Turbidity currents and their deposits. Annu. Rev. Fluid Mech. **42**, 135 (2010)
6. Faillettaz, J., Louchet, F., Grasso, J.R.: Two-threshold model for scaling laws of noninteracting snow avalanches. Phys. Rev. Lett. **93**, 208001 (2004)
7. Hopfinger, E.J.: Snow avalanche motion and related phenomena. Annu. Rev. Fluid Mech. **15**, 47 (1983)
8. Hall, F.F., Neff, W.D., Frazier, T.V.: Wind shear observations in thunderstorm density currents. Nature **264**, 408 (1976)
9. Simpson, J.E.: Gravity currents in the laboratory, atmosphere and oceans. Annu. Rev. Fluid Mech. **14**, 213 (1982)
10. Huppert, H.E.: Gravity currents: a personal perspective. J. Fluid Mech. **554**, 299 (2006)
11. von Karman, R.: The engineer grapples with nonlinear problems. Bull. Am. Math. Soc. **46**, 615 (1940)
12. Benjamin, T.B.: Density currents and related phenomena. J. Fluid Mech. **31**, 209 (1968)
13. Hallworth, M.A., Huppert, H.E., Ungarish, M.: Axisymmetric gravity currents in a rotating system: experimental and numerical investigations. J. Fluid Mech. **447**, 1 (2001)
14. Huq, P.: The role of aspect ratio on entrainment rates of instantaneous, axisymmetric finite volume releases of density fluid. J. Hazard. Mater. **49**, 89 (1996)
15. Huppert, H.E., Simpson, J.E.: The slumping of gravity currents. J. Fluid Mech. **99**, 785 (1980)
16. Cantero, M., Lee, J., Balachandar, S., García, M.: On the front velocity of gravity currents. J. Fluid Mech. **586**, 1 (2007)
17. Zemach, T., Ungarish, M.: Gravity currents in non-rectangular cross-section channels: analytical and numerical solutions of the one-layer shallow-water model for high-Reynolds-number propagation. Phys. Fluids **25**, 026601 (2013)
18. Rottman, J.W., Simpson, J.E.: Density currents produced by instantaneous releases of a heavy fluid in a rectangular channel. J. Fluid Mech. **135**, 95 (1983)
19. Klemp, J.B., Rotunno, R., Skamarock, W.C.: On the dynamics of density currents in a channel. J. Fluid Mech. **269**, 169 (1994)
20. Cantero, M., Balachandar, S., García, M., Bock, D.: Turbulent structures in planar gravity currents and their influence on the flow dynamics. J. Geophys. Res. Oceans **113**, C08018 (2008)
21. Lighthill, J.: Waves in Fluids. Cambridge University Press, Cambridge (1978)
22. Sachdev, P.L.: Shock Waves and Explosions. Chapman & Hall/CRC, London (2004)
23. Ungarish, M.: An Introduction to Gravity Currents and Intrusions. CRC Press, Boca Raton (2009)
24. Cantero, M., Balachandar, S., Garcia, M.: High-resolution simulations of cylindrical density currents. J. Fluid Mech. **590**, 437 (2007)
25. Simpson, J.E.: Effect of the lower boundary on the head of a gravity current. J. Fluid Mech. **53**, 759 (1972)
26. La Rocca, M., Adduce, C., Sciortino, G., Pinzon, A.B.: Experimental and numerical simulation of three-dimensional gravity currents on smooth and rough bottom. Phys. Fluids **20**, 106603 (2008)